RESEARCH ARTICLE

A local differential quadrature method for the generalized nonlinear Schrödinger (GNLS) equation

Meirikim Panmei[a,*], Roshan Thoudam[a]

[a]*Department of Mathematics, Manipur University, Canchipur - 795003, Manipur, India*
 meirikimp@gmail.com, roshandmc@gmail.com

ARTICLE INFO	ABSTRACT
	A local differential quadrature method based on Fourier series expansion numerically solves the generalized nonlinear Schrödinger equation. For time integration, a Runge-Kutta fourth-order method is used. Matrix stability analysis is used to examine the method's stability. Three test problems involving the motion of a single solitary wave, the interaction of two solitary waves, and a solution that blows up in finite time, respectively, demonstrate the accuracy and efficiency of the provided method. Finally, the numerical results obtained from the presented method are compared with the exact solution and those obtained in earlier works available in the literature.

1. Introduction

We consider the generalized nonlinear Schrödinger (GNLS) equation, given by

$$i\omega_t + \omega_{xx} + q_1|\omega|^2\omega + q_2|\omega|^4\omega + \\ iq_3(|\omega|^2)_x\omega + iq_4|\omega|^2\omega_x = 0, \tag{1}$$

where $i = \sqrt{-1}$, ω is a complex-valued function of the spatial coordinate x and time t. The subscripts t and x denote differentiation with respect to time, t and space, x and q_1, q_2, q_3, q_4 are real parameters. Eq.(1) describes the modulation of a quasi-monochromatic wave train in a weakly nonlinear dispersive medium [1]. It also describes the behaviour of the Stokes wave near the state of modulation instability, which was independently proposed by Johnson [2], Kakutani and Michihiro [3]. The GNLS Eq.(1) takes some special forms [1] and these forms have found many applications [1, 4]. One of the special forms of Eq.(1) is the well known cubic nonlinear Schrödinger (CNLS) equation:

$$i\omega_t + \omega_{xx} + q_1|\omega|^2\omega = 0, \tag{2}$$

which has found applications in nonlinear optics [5], plasma physics [6] and fluid dynamics [7]. Other special forms of Eq.(1) have applications including propagation of nonlinear Alfvên waves [8] and the self-modulation of the complex amplitude of the solution to the Benjamin-Ono equation [9]. Under the condition that the initial condition $\omega(x, 0)$ vanishes for sufficiently large x, the CNLS Eq.(2) has analytic solution given by [6,10]. There are many papers about the numerical and analytical solutions of the CNLS equation. However, a few papers can be found in the past about the numerical and analytical solutions of the GNLS equation. Exact solution of the GNLS equation was obtained by using Gauss transformation by Pathria and Morris [1]. They also obtained the numerical solution of the GNLS equation using the pseudo-spectral split-step method. Different

---

*Corresponding Author

split-step pseudo-spectral methods were implemented for the numerical solution of the GNLS equation by Pathria and Morris [4]. Muslu and Erbay [11] used first, second and fourth-order versions of the split-step Fourier method to solve the GNLS equation numerically. The quintic B-spline collocation method was used to solve the GNLS equation by Irk and Dağ [12]. A meshfree method based on RBFs has been used to solve the GNLS equation by Uddin and Haq [13]. Bashan, Ali, et al. [14–16] used various methods based on the differential quadrature method to find the solution of the nonlinear Schödinger Equation. In literature, [17–19], many researchers have developed various types of differential quadrature methods (DQM) using different base functions.

Assuming that ω and all its derivatives tend to zero rapidly as $x \to \pm\infty$, the solutions of the GNLS equation possess the following conservation laws [1, 4]:

$$I_1 = \int_{-\infty}^{\infty} |\omega|^2 dx, \tag{3}$$

$$
\begin{aligned}
I_2 = \int_{-\infty}^{\infty} &\left[|\omega_x|^2 - \frac{1}{2}(2q_3 + q_4)|\omega|^2 Im(\omega\bar{\omega}_x) \right. \\
&\left. - \frac{1}{2}q_1|\omega|^4 + \frac{1}{6}\{q_3(2q_3 + q_4) - 2q_2\}|\omega|^6 \right] dx,
\end{aligned}
\tag{4}
$$

and

$$I_3 = \int_{-\infty}^{\infty} \left[2Im(\omega\bar{\omega}_x) - q_3|\omega|^4 \right] dx, \tag{5}$$

which are the conservation of mass, energy and impulse respectively.

The differential quadrature method (DQM) was first introduced by Bellman et al. [20] in 1972 as a simple and versatile numerical technique for solving complex differential equations. This method approximates a function's derivative at a certain point through a weighted linear sum of the functional values at specific collocation points, whereby a key aspect is related to the computation of weighting coefficients. Many authors have used various test functions to formulate various DQ methods, like Legendre polynomials, Lagrange interpolating polynomials, spline functions, radial basis functions (RBF), Chebyshev polynomials, etc. [20–26]. Shu proposed a better method for computing weighting coefficients [27]. Shu and Richards [28] used Lagrange interpolating polynomials, which have no limitation on the choice of grid points. This leads to the polynomial-based differential quadrature (PDQ) method. They also obtained a recurrence

formula to compute the weighting coefficients for higher-order derivatives. When using Fourier series expansion, we call it the Fourier-based differential quadrature (FDQ) method.

The main advantage of DQM is their high accuracy. In general, DQMs are global in nature [29], which means that they approximate a function and its derivative at a point by using the functional values at all collocation points in the domain. The number of collocation points in the given domain must be large enough to achieve high accuracy approximation. However, it was found that DQM is inefficient when the number of collocation points is larger [30] because of instability. In this regard, Zong and Lam [31] introduced a localized DQ method to keep a balance between stability and accuracy. It has been demonstrated that accuracy and stability can be balanced by approximating the derivative of a function at a position using a weighted sum of functional values at the points in its neighbourhood rather than all collocation points. Therefore, we proposed an efficient numerical approach based on the local differential quadrature method using Fourier series expansion to solve the GNLS Eq.(1).

The paper is organized as follows: Section 2 briefly introduces DQM and the local Fourier-based differential quadrature (L-FDQ) method. The L-FDQ method is implemented in section 3 to solve the GNLS equation. In section 4, we discuss the matrix stability analysis of the proposed method. Section 5 reports the numerical results of the GNLS equation for some test problems. In section 6, we draw a brief conclusion about the presented method.

2. Differential quadrature method (DQM)

DQM is an approximation to the derivative of a function at any grid point using the weighted linear sum of all functional values at certain collocation points in the given domain of definition. We consider an arbitrarily distributed N grid points $x_1 < x_2 < \cdots < x_N$ on the real axis. Then, according to DQ discretization, the nth order derivatives of $U(x, t)$ w.r.t. the spatial coordinate x at a point x_i is given by

$$U^{(n)}(x_i, t) = \sum_{j=1}^{N} w_{i,j}^{(n)} U(x_j, t), \tag{6}$$

where $w_{i,j}^{(n)}$ represents the weighting coefficients, $i, j = 1, \ldots, N$ and $n = 1, \ldots, N-1$.

2.1. Fourier-based differential quadrature (FDQ)

For Fourier-based differential quadrature (FDQ), we consider an arbitrary function defined on the interval $[a, b]$. Two typical sets of base functions are used to compute the weighting coefficients. These sets of base functions are:

$$1, \cos\left(\frac{\pi x}{b-a}\right), \sin\left(\frac{\pi x}{b-a}\right), \ldots,$$
$$\cos\left(\frac{(N-1)\pi x}{2(b-a)}\right), \sin\left(\frac{(N-1)\pi x}{2(b-a)}\right), \tag{7}$$

and

$$g_j(x) = \frac{G(x)}{\sin\left(\frac{\pi(x-x_j)}{2(b-a)}\right) G^{(1)}(x_j)}, \quad x \in [a,b], \tag{8}$$
$$j = 1, 2, \ldots, N$$

where

$$G(x) = \prod_{k=1}^{N} \sin\left(\frac{\pi(x-x_k)}{2(b-a)}\right),$$

$$G^{(1)}(x_j) = \prod_{k=1, k \neq j}^{N} \sin\left(\frac{\pi(x_j-x_k)}{2(b-a)}\right), \quad x \in [a,b],$$

$$j = 1, \ldots, N.$$

Using these sets of base functions given in Eq.(7) and Eq.(8), the weighting coefficients for the first and second-order derivatives as evaluated by Shu [29] are as follows:

$$\left.\begin{aligned}
&w_{i,j}^{(1)} = \frac{\pi}{2(b-a)} \frac{G^{(1)}(x_i)}{\sin\left(\frac{\pi(x_i-x_j)}{2(b-a)}\right) G^{(1)}(x_j)}, \; i \neq j, \\
&w_{i,j}^{(2)} = w_{i,j}^{(1)}\left(2w_{i,i}^{(1)} - \frac{\pi}{(b-a)}\cot\left(\frac{\pi(x_i-x_j)}{2(b-a)}\right)\right), \\
&i \neq j, \\
&w_{i,i}^{(n)} = -\sum_{j=1, j \neq i}^{N} w_{i,j}^{(n)}, \; n = 1, 2
\end{aligned}\right\} \tag{9}$$

where $i, j = 1, 2, \ldots, N$. We used equally spaced grid points in the space direction to approximate the derivative of the unknown function.

2.2. Local Fourier-based differential quadrature (L-FDQ)

We consider a partition $a = x_1 < x_2 < \cdots < x_i < \cdots < x_N = b$ of the domain $[a,b]$. Following the method adopted by Shu [27], we consider a location x_i ($i = 1, 2, \ldots, N$) and for each i, consider a stencil $S_i = \{x_{i-K_1}, x_{i-K_1+1}, \ldots, x_{i-1}, x_i, x_{i+1}, \ldots x_{i+K_2}\}$ containing $K+1$ ($K = K_1 + K_2$) grid points. For the left boundary point $x_1, K_1 = 0, K_2 = K$, while for the right boundary point $x_N, K_1 = K, K_2 = 0$. Then using the $K+1$ grid points $x_{i-K_1}, x_{i-K_1+1}, \ldots, x_{i-1}, x_i, x_{i+1}, \ldots x_{i+K_2}$ the nth order partial derivative of the function $U(x,t)$ with respect to x at x_i is given by

$$U_x^{(n)}(x_i, t) = \sum_{j=-K_1}^{K_2} w_{i,i+j}^{(n)} U(x_{i+j}, t) \tag{10}$$

where , the L-FDQ weighting coefficients for the first and second-order derivatives in Eq.(9) are given by

$$w_{i,i+j}^{(1)} = \frac{\pi}{2(b-a)} \frac{G^{(1)}(x_i)}{\sin\left(\frac{\pi(x_i-x_{i+j})}{2(b-a)}\right) G^{(1)}(x_{i+j})},$$
$$\text{for } j \neq 0, j = -K_1, \ldots, K_2 \tag{11}$$

where

$$G^{(1)}(x_i) = \prod_{\substack{k=K_1 \\ k \neq 0}}^{K_2} \sin\left(\frac{\pi(x_i - x_{i+k})}{2(b-a)}\right) \text{ and}$$

$$G^{(1)}(x_{i+j}) = \prod_{\substack{k=-K_1 \\ k \neq j}}^{K_2} \sin\left(\frac{\pi(x_{i+j} - x_{i+k})}{2(b-a)}\right),$$

and

$$w_{i,i+j}^{(2)} = w_{i,i+j}^{(1)}\left(2w_{i,i}^{(1)} - \frac{\pi}{b-a}\cot\left(\frac{\pi(x_i-x_{i+j})}{2(b-a)}\right)\right),$$
$$j \neq 0, j = -K_1, \ldots, K_2. \tag{12}$$

For the diagonal coefficients $w_{i,i}^{(n)}$, we have

$$w_{i,i}^{(n)} = -\sum_{\substack{k=-K_1, \\ k \neq 0}}^{K_2} w_{i,i+k}^{(n)} \quad ; n = 1, 2. \tag{13}$$

Once the weighting coefficients are computed, then we make the following differentiation matrices, $\mathbf{W}^{(1)} = \left(w_{i,j}^{(1)}\right)_{N \times N}$ and $\mathbf{W}^{(2)} = \left(w_{i,j}^{(2)}\right)_{N \times N}$ to approximate the first and second-order spatial

derivatives of $U(x,t)$ in the domain $[a,b]$. These differentiation matrices are banded.

3. Implementation of L-FDQ

The GNLS Eq.(1) is examined in this part, with the following initial and boundary conditions applied across the interval $[a,b]$:

$$\omega(x,0) = f(x), x \in [a,b] \tag{14}$$
$$\omega(a,t) = \omega(b,t) = 0, t \in (0,T]. \tag{15}$$

Taking $\omega(x,t) = u(x,t) + iv(x,t)$, where $i = \sqrt{-1}$ the GNLS Eq.(1) with the initial and boundary conditions (14) and (15) are transformed into the following coupled initial-boundary value problem (IBVP):

PDEs:

$$\left. \begin{aligned} u_t =& - v_{xx} - [q_1(u^2 + v^2) + q_2(u^2 + v^2)^2]v \\ & - [2q_3u^2 + q_4(u^2 + v^2)]u_x - 2q_3uvv_x \\ v_t =& \ u_{xx} + [q_1(u^2 + v^2) + q_2(u^2 + v^2)^2]u \\ & - [2q_3v^2 + q_4(u^2 + v^2)]v_x - 2q_3uvu_x \end{aligned} \right\} \tag{16}$$

$$\text{ICs}: u(x,0) = f_u(x), v(x,0) = f_v(x), x \in [a,b] \tag{17}$$

$$\text{BCs}: u(a,t) = u(b,t) = 0, v(a,t) = v(b,t) = 0,$$
$$t \in (0,T]. \tag{18}$$

To solve the system (16) with ICs (17) and BCs (18) at the collocation points $\{x_1, x_2, \ldots, x_N\}$ with uniform step size $h = x_{i+1} - x_i$, for $i = 1, 2, \ldots, N-1$ we define the following:

$$\mathbf{U}(t) = [u_1(t), u_2(t), \ldots, u_N(t)]^T,$$

$$\mathbf{V}(t) = [v_1(t), v_2(t), \ldots, v_N(t)]^T,$$

where $u_i(t) = u(x_i,t), v_i(t) = v(x_i,t)$ for all $i = 1, 2, \ldots, N$.

Using these definitions and the differentiation matrices $\mathbf{W}^{(1)}$ and $\mathbf{W}^{(2)}$ as defined in section 3, the system of PDEs (16) reduces to the following system of ordinary differential equations (ODEs), which can be written in the following matrix form:

$$\left. \begin{aligned} \mathbf{U}'(t) =& - \mathbf{W}^{(2)} \cdot \mathbf{V}(t) - \left[q_1\left(\mathbf{U}^2(t) + \mathbf{V}^2(t)\right) + \right. \\ & \left. q_2\left(\mathbf{U}^2(t) + \mathbf{V}^2(t)\right)^2\right] * \mathbf{V}(t) \\ & - \left[2q_3\mathbf{U}^2(t) + q_4\left(\mathbf{U}^2(t) + \mathbf{V}^2(t)\right)\right] * \\ & \left(\mathbf{W}^{(1)} \cdot \mathbf{U}(t)\right) - 2q_3\mathbf{U}(t) * \mathbf{V}(t) * \left(\mathbf{W}^{(1)} \cdot \mathbf{V}(t)\right) \\ \mathbf{V}'(t) =& \ \mathbf{W}^{(2)} \cdot \mathbf{U}(t) + \left[q_1\left(\mathbf{U}^2(t) + \mathbf{V}^2(t)\right) + \right. \\ & \left. q_2\left(\mathbf{U}^2(t) + \mathbf{V}^2(t)\right)^2\right] * \mathbf{U}(t) \\ & - \left[2q_3\mathbf{V}^2(t) + q_4\left(\mathbf{U}^2(t) + \mathbf{V}^2(t)\right)\right] * \\ & \left(\mathbf{W}^{(1)} \cdot \mathbf{V}(t)\right) - 2q_3\mathbf{U}(t) * \mathbf{V}(t) * \left(\mathbf{W}^{(1)} \cdot \mathbf{U}(t)\right) \end{aligned} \right\} \tag{19}$$

where " $\cdot$ " indicates the multiplication of two matrices and $\mathbf{U}(t) * \mathbf{V}(t)$, $\mathbf{U}^2(t) = \mathbf{U}(t) * \mathbf{U}(t)$ denote the component by component multiplication of two matrices.

Using the corresponding ICs and BCs (17) and (18), we solve the above system of ODEs (19) by the usual RK4 method.

4. Stability analysis

The method's stability is analyzed using the matrix stability analysis as suggested in literature [30,32]. After linearization of the system of ODEs (19), the resulting system can be written in the following matrix form:

$$\mathbf{X}'(t) = \mathbf{A} \cdot \mathbf{X}(t) \tag{20}$$

(since, both the system of ODEs and the BCs are homogeneous) or

$$\begin{bmatrix} \mathbf{U}'(t) \\ \mathbf{V}'(t) \end{bmatrix}$$
$$= \begin{bmatrix} -\alpha\mathbf{W}^{(1)} & -\beta\mathbf{I} - \gamma\mathbf{W}^{(1)} - \mathbf{W}^{(2)} \\ \beta\mathbf{I} - \gamma\mathbf{W}^{(1)} + \mathbf{W}^{(2)} & -\alpha\mathbf{W}^{(1)} \end{bmatrix} \begin{bmatrix} \mathbf{U}(t) \\ \mathbf{V}(t) \end{bmatrix}$$

where $\mathbf{I}$ is the identity matrix of order $N \times N$, $\mathbf{W}^{(1)}$ and $\mathbf{W}^{(2)}$ are the weighting coefficient matrices for first and second order derivatives respectively, as defined in section-3. Also, we have taken $\alpha = 2q_3\bar{u}^2 + q_4(\bar{u}^2 + \bar{v}^2)$, $\beta = q_1(\bar{u}^2 + \bar{v}^2) + q_2(\bar{u}^2 + \bar{v}^2)^2$ and $\gamma = 2q_3\bar{u}\bar{v}$, where $\bar{u} = ||\mathbf{U}||_\infty$ and $\bar{v} = ||\mathbf{V}||_\infty$.
The stability region for the complex eigenvalues is shown in Figure 1 [33].
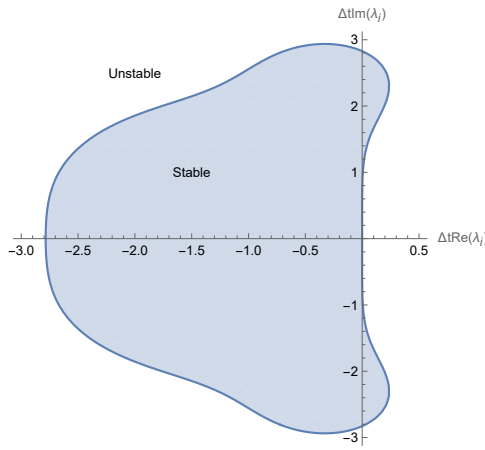
Figure 1. Stability region for complex eigenvalues.

The stability of the numerical integration of the system (20) is related to the stability of the numerical scheme for solving it. If the system of ODEs in (20) is not stable, then the stable numerical scheme for temporal discretization may not generate the converged solution.

The stability of (20) depends on the eigenvalues of the coefficient matrix $\mathbf{A}$ since its exact solution can be found using the eigenvalues. Let λ_i be the eigenvalues of the coefficient matrix $\mathbf{A}$, then the stable solution of $\mathbf{X}(t)$ as $t \to \infty$ requires:

(1) if all the eigenvalues are real $-2.78 < \Delta t \, \lambda_i < 0$
(2) if eigenvalues are imaginary, $-2\sqrt{2} < \Delta t \, \lambda_i < 2\sqrt{2}$
(3) if eigenvalues are complex $\Delta t \, \lambda_i$ should be in the region shown in Figure 1

At the end of section 5, we will calculate the eigenvalues of the coefficient matrix $\mathbf{A}$ and we will see that our scheme is stable with the proper choice of the time step Δt.

5. Numerical experiment

The accuracy and effectiveness of the present method are demonstrated by taking three test problems. The accuracy of the method is measured by using $L_\infty-$ error norm, which is defined as

$$L_\infty = \Big\| \, |\omega|_{exct} - |\omega|_{approx} \, \Big\|_\infty$$
$$= \max_{1 \le i \le N} \Big| \, |\omega(i)|_{exct} - |\omega(i)|_{approx} \Big|$$

5.1. Single solitary wave solution

The exact solitary wave solution of the GNLS Eq.(1) for the parameters $q_1 = 0.5$, $q_2 = -1.75$, $q_3 = -1.0$ and $q_4 = -2.0$ is given by [1, 4]:

$$\omega(x,t) = \frac{2e^{i\phi(x,t)}}{\sqrt{4 + 3\sinh^2(x - 2t - x_0)}}, \tag{21}$$

where $\phi(x,t) = 2\tanh^{-1}\left[\frac{1}{2}\tanh(x - 2t - x_0)\right] + x - x_0$.

The modulus of the above solution represents a single solitary wave initially located at x_0, moving to the right with constant speed 2. The exact values of the three conserved quantities I_1, I_2 and I_3 as given in Eq.(3)-Eq.(5), for this problem can be found as:

$$\left.\begin{aligned} I_1 &= 2\log 3 \approx 2.19722, \\ I_2 &= -1.5 + 3.875\log 3 \approx 2.75712, \\ I_3 &= 4 - 9\log 3 \approx -5.88751. \end{aligned}\right\} \tag{22}$$

Table 1. $L_\infty-$ errors and conserved quantities for different stencil sizes K, for a single solitary wave motion, when $h = 0.1$, $\Delta t = 0.001$ over the domain $-20 \le x \le 30$.

| K	I_1	I_2	I_3	L_∞
2	2.19724	2.75715	-5.88743	2.40377×10^{-2}
4	2.19712	2.75701	-5.88717	1.26695×10^{-3}
6	2.19712	2.75701	-5.88717	1.07408×10^{-4}
8	2.19712	2.75701	-5.88717	9.39029×10^{-6}
10	2.19712	2.75701	-5.88717	4.23275×10^{-6}
12	2.19712	2.75701	-5.88717	9.42336×10^{-6}

Using the initial condition obtained from (21) and imposing the boundary conditions (18), the GNLS equation is simulated by the proposed method for different stencils over the solution domain $[-20, 30]$. The $L_\infty-$ error and the three conserved quantities for different stencil sizes K are reported in Table 1. From Table 1, we observe that $L_\infty-$ error decreases when K, the size of the stencil increases from $K = 2$ to $K = 10$, however $L_\infty-$ increase when K reached 12 .

Table 2. Comparison of $L_\infty-$ error at $T = 3$, for a single solitary wave motion, with $x_0 = 15$, $N = 513$, $K = 18$ and $-20 \le x \le 60..$

| Δt	Present Method	Collocation [12]	First Order [11]	Second Order [11]
0.010	2.75032×10^{-5}	3.0×10^{-4}	3.1×10^{-3}	3.0×10^{-5}
0.005	5.65732×10^{-6}	3.1×10^{-5}	1.6×10^{-3}	2.0×10^{-5}
0.001	3.86334×10^{-7}	2.1×10^{-6}	3.1×10^{-4}	8.0×10^{-7}

Table 3. $L_\infty-$ error norms and Rate of Convergence (ROC) for various numbers of grid points for $K = 6$, $K = 8$ and $K = 10$ with $\Delta t = 0.001$ at $T = 5$.

N	$K = 6$		$K = 8$		$K = 10$	
	Error	*ROC*	*Error*	*ROC*	*Error*	*ROC*
201	1.83495×10^{-2}	$-$	1.01788×10^{-2}	$-$	6.13463×10^{-3}	$-$
301	1.98217×10^{-3}	5.5111	4.52132×10^{-4}	7.71185	1.13554×10^{-4}	9.87958
401	3.91842×10^{-4}	5.65132	5.23908×10^{-5}	7.51345	7.34062×10^{-6}	9.548
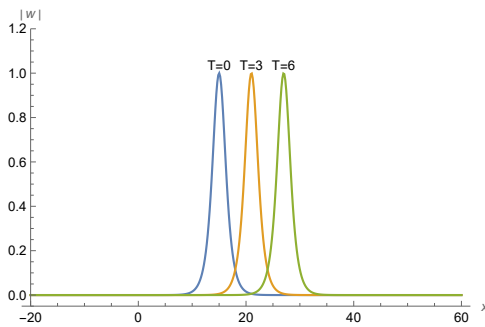
Figure 2. Motion of a single solitary wave at different time levels.
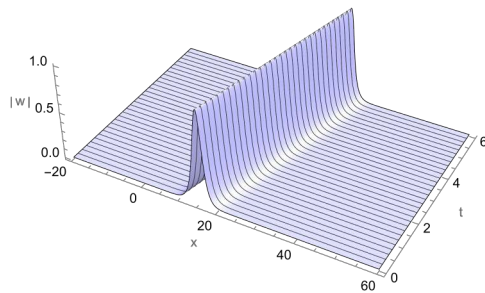
Figure 3. Space time graph of a single solitary wave for GNLS equation ($N = 513, K = 18, \Delta t = 0.001$)

In order to compare our result with [11, 12], we choose $x_0 = 15$, $N = 513$ over the space interval $[-20, 60]$ with time step size, $\Delta t = 0.001$. This comparison is reported in Table 2. Figure 2 and 3 represent the space-time graph of the numerical solution of single solitary wave up to time $T = 6$.

The absolute error distribution at time $T = 6$ for this case is shown in Figure 4.

The numerical rate of convergence (ROC) is calculated by using the formula [33],

$$ROC \approx \frac{\ln\left(\frac{E(N_2)}{E(N_1)}\right)}{\ln\left(\frac{N_1}{N_2}\right)}$$

where $E(N_i)$ is the $L_\infty-$ error norm when using N_i grid points.

The $L_\infty-$ error norm and numerical rate of convergence analysis for various number of grid points are shown in Table 3. From the table it is evident that the rate of convergence (ROC) depends on the value of K.

5.2. Interaction of two solitons

In this test problem, we consider the interaction of two solitons for the GNLS equation, in which the coefficients are taken as $q_1 = 1$, $q_2 = 1$, $q_3 = -2$ and $q_4 = 0$. With these coefficients, we take the initial conditions as given by [1, 4] :

$$\omega(x, 0) = \omega_1(x, 0) + \omega_2(x, 0), \qquad (23)$$

where

$$\omega_1(x, 0) = \frac{1}{\sqrt{2}} \operatorname{sech}\left[\frac{1}{2}(x - 15)\right]$$
$$e^{i\left[\frac{1}{4}(x-15)+\tanh\{\frac{1}{2}(x-15)\}\right]},$$

and

$$\omega_2(x, 0) = \frac{1}{2\sqrt{2}} \operatorname{sech}\left[\frac{1}{4}(x - 35)\right]$$
$$e^{i\left[-\frac{1}{2}(x-35)+\frac{1}{2}\tanh\{\frac{1}{4}(x-35)\}\right]}.$$

Table 4. Conserved quantities at different time levels, for interaction of two solitons over the space interval $[-50, 100]$ with $N = 501$ and $\Delta t = 0.001$ with stencil size $K = 14$.

T	I_1	I_2	I_3
0	3.00145	0.18974	-1.02223×10^{-4}
5	3.00139	0.18977	-1.02687×10^{-4}
10	3.00141	0.18986	-1.02482×10^{-4}
15	3.00154	0.18968	-1.02161×10^{-4}
20	3.00142	0.18975	-1.02403×10^{-4}

The exact values of the conserved quantities for this problem are $I_1 = 3.0$, $I_2 = \frac{3}{16}$ and $I_3 = 0.0$. The initial condition defined in Eq.(23), represents two solitons, one initially located at $x_1 = 15$, moving to the right with speed $\frac{1}{2}$ and having amplitude $\frac{1}{\sqrt{2}}$ and another initially located at $x_2 = 35$ moving to the left with unit speed and having amplitude $\frac{1}{2\sqrt{2}}$. We have simulated this problem with the present method. These two solitons interact, and after the interaction, they retain their shapes and speeds, which has been shown in Figure 5. In Table 4, the conserved quantities I_1, I_2 and I_3 at different time levels are reported. From the table, we see that the variations of these conserved quantities from the exact values are negligible.
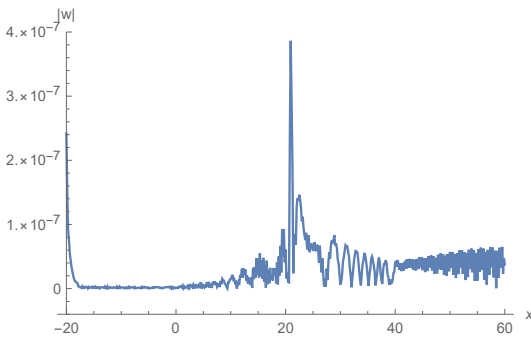
Figure 4. Error distribution of a single solitary wave for GNLS equation at t=6, ($N = 513, K = 18, \Delta t = 0.001$).
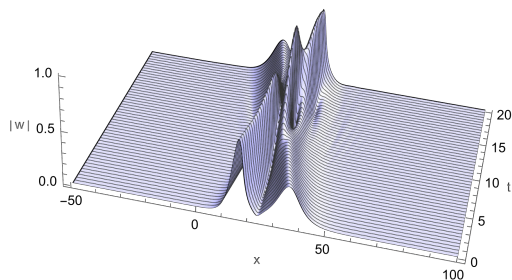

Figure 5. Interaction of two solitons ($N = 501, K = 14, \Delta t = 0.001$).

5.3. Blow-up

In [1], it has been reported that for specific values of the coefficients and for certain initial conditions, the solutions of the GNLS equation have finite time blow-up. To see this experience, we take $q_1 = -2$, $q_2 = 20$ and $q_3 = q_4 = 0$ and the Gaussian function $\omega(x, 0) = e^{-x^2}$ as the initial condition, the numerical simulation has been conducted by our method. The exact values of the conserved quantities for this problem are found to be $I_1 = \sqrt{\pi/2} \approx 1.5331$, $I_2 = \sqrt{\pi}(9\sqrt{2} + 9 - 20\sqrt{6})/18 \approx -2.68447$ and $I_3 = 0$.

Table 5. Conserved quantities at different time levels for case of finite time blow-up ($N = 151$, $-7.5 \leq x \leq 7.5$, $\Delta t = 10^{-4}$ and $K = 6$).

| T	I_1	I_2	I_3
0.00	1.25330	-2.68419	0.0
0.02	1.25329	-2.68414	-4.40186×10^{-17}
0.06	1.25107	-2.34227	-1.13798×10^{-15}
0.07	1.15379	-2.07551	-6.16625×10^{-14}
0.08	1.24722	-2.63257	3.98570×10^{-14}
0.10	1.25129	-2.88368	5.09393×10^{-14}
0.15	1.10587	-2.23570	-6.12399×10^{-12}
0.20	1.24751	-3.39736	1.97811×10^{-11}
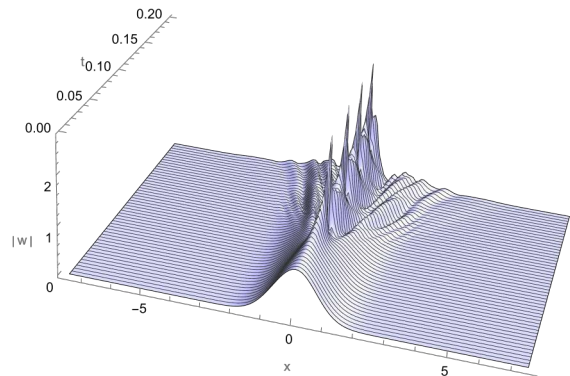
Figure 6. Finite time blow-up, with initial condition $\omega(x, 0) = e^{-x^2} (-7.5 \leq x \leq 7.5, N = 151, \Delta t = 0.0001, K = 12)$.

The conserved quantities for this problem have been reported in Table 5, and from the table, we see that the variation of the conserved quantity is more in I_2. Figure 6 shows the space-time graph of this test problem. According to [1], it has been shown that the exact solution $\omega(x, t)$ for this problem will blow up in finite time, and an upper bound on the blow-up time is $t \approx 1.7$. However, from Figure 6, we observed that the blow-up

is evident at $t = 0.07$, and this result is consistent with the result obtained using the quintic b-spline collocation method in [12]. Also, the graph shows that the blow-up is well occurring at about $t = 0.07, 0.11, 0.15$ and 0.20.

As a part of the stability analysis, we have calculated the eigenvalues of the coefficient matrix, **A** as defined in Eq.(20). We take $\bar{u} = \bar{v} = 1$, so that $\alpha = 2q_3 + 2q_4$, $\beta = 2q_1 + 4q_2$ and $\gamma = 2q_3$. The maximum absolute values of the eigenvalues of the coefficient matrix **A** for a single solitary wave motion is determined to be 248.273 ($N = 513$). Therefore, for maintaining stability the maximum value of Δt is given by $\Delta t < \frac{2\sqrt{2}}{248.273} = 0.0113924$. However, we take smaller values of Δt in order to get more accurate results. The distribution of eigenvalues for this case is shown in Figure 7. The figure shows that more eigenvalues are distributed near the imaginary axis.
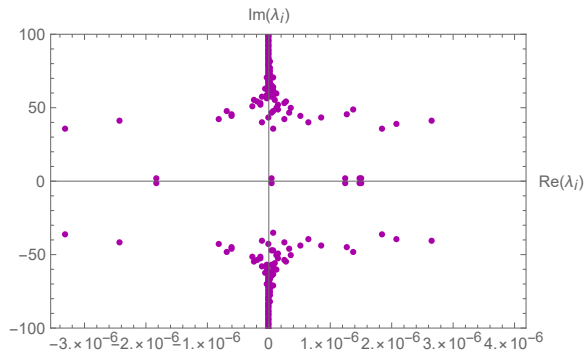
Figure 7

Distribution of eigenvalues for the coefficient matrix, **A** ($N = 513, K = 12$).

6. Conclusion

In this study, we have examined the numerical solution of the GNLS equation by means of the L-FDQ method. The GNLS equation is discretized in space using differentiation matrices obtained from the L-FDQ method, and the resulting system of ordinary differential equations in time t is solved by the usual RK4 method. By the present method, the motion of a single solitary wave has been investigated, and the results obtained are compared with the exact solution and some other results obtained in earlier works. It has also been studied how two solitons interact, and it has been found that after the encounter, the solitons maintained their identities. The finite time blow-up problem has also been tackled by the suggested approach, which is consistent with the previous findings. Further, this study found that the finite time blow-up is repeating.

References

[1] Pathria, D., & Morris, J. L. (1989). Exact solutions for a generalized nonlinear Schrödinger equation. *Physica Scripta*, 39(6), 673-679. `https://doi.org/10.1088/0031-8949/39/6/001`

[2] Johnson, R. S. (1977). On the modulation of water waves in the neighbourhood of kh ≈ 1.363. Proceedings of the Royal Society of London. A. Mathematical and Physical Sciences, 357(1689), 131-141. `https://doi.org/10.1098/rspa.1977.0159`

[3] Kakutani, T., & Michihiro, K. (1983). Marginal State of Modulational Instability-Note on Benjamin-Feir Instability. *Journal of the Physical Society of Japan*, 52(12), 4129-4137. `https://doi.org/10.1143/JPSJ.52.4129`

[4] Pathria, D., & Morris, J. L. (1990). Pseudo-spectral solution of nonlinear Schrödinger equations. *Journal of Computational Physics*, 87(1), 108-125. `https://doi.org/10.1016/0021-9991(90)90228-S`

[5] Strauss, W. A. (1978). The nonlinear Schrödinger equation. In North-Holland Mathematics Studies (Vol. 30, pp. 452-465). North-Holland. `https://doi.org/10.1016/S0304-0208(08)70877-6`

[6] Shabat, A., & Zakharov, V. (1972). Exact theory of two-dimensional self-focusing and one-dimensional self-modulation of waves in nonlinear media. *Soviet Physics JETP*, 34(1), 62.

[7] Hasimoto, H., & Ono, H. (1972). Nonlinear modulation of gravity waves. *Journal of the Physical Society of Japan*, 33(3), 805-811. `https://doi.org/10.1143/JPSJ.33.805`

[8] Kaup, D. J., & Newell, A. C. (1978). An exact solution for a derivative nonlinear Schrödinger equation. *Journal of Mathematical Physics*, 19(4), 798-801. `https://doi.org/10.1063/1.523737`

[9] Tanaka, M. (1982). Nonlinear self-modulation problem of the Benjamin-Ono equation. *Journal of the Physical Society of Japan*, 51(8), 2686-2692. `https://doi.org/10.1143/JPSJ.51.2686`

[10] Karpman, V. I., & Krushkal, E. M. (1969). Modulated waves in nonlinear dispersive media. *Soviet Journal of Experimental and Theoretical Physics*, 28, 277.

[11] Muslu, G. M., & Erbay, H. A. (2005). Higher-order split-step Fourier schemes for

the generalized nonlinear Schrödinger equation.*Mathematics and Computers in Simulation*, 67(6), 581-595. `https://doi.org/10.1016/j.matcom.2004.08.002`

[12] Irk, D., & Dağ, İ. (2011). Quintic B-spline collocation method for the generalized nonlinear Schrödinger equation. *Journal of the Franklin Institute*, 348(2), 378-392. `https://doi.org/10.1016/j.jfranklin.2010.12.004`

[13] Uddin, M., & Haq, S. (2013). On the numerical solution of generalized nonlinear Schrodinger equation using radial basis functions. *Miskolc Mathematical Notes*, 14(3), 1067-1084. `https://doi.org/10.18514/MMN.2013.486`

[14] Başhan, A. (2019). A mixed methods approach to Schrödinger equation: Finite difference method and quartic B-spline based differential quadrature method. *An International Journal of Optimization and Control: Theories & Applications (IJOCTA)*, 9(2), 223-235. `https://doi.org/10.11121/ijocta.01.2019.00709`

[15] Bashan, A., Yagmurlu, N. M., Ucar, Y., & Esen, A. (2017). An effective approach to numerical soliton solutions for the Schrödinger equation via modified cubic B-spline differential quadrature method. *Chaos, Solitons & Fractals*, 100, 45-56. `https://doi.org/10.1016/j.chaos.2017.04.038`

[16] Başhan, A., Uçar, Y., Murat Yağmurlu, N., & Esen, A. (2018). A new perspective for quintic B-spline based Crank-Nicolson-differential quadrature method algorithm for numerical solutions of the nonlinear Schrödinger equation. *The European Physical Journal Plus*, 133(1), 12. `https://doi.org/10.1140/epjp/i2018-11843-1`

[17] Uçar, Y., Yağmurlu, M., & Başhan, A. (2019). Numerical solutions and stability analysis of modified Burgers equation via modified cubic B-spline differential quadrature methods. *Sigma Journal of Engineering and Natural Sciences*, 37(1), 129-142.

[18] Başhan, A., Yağmurlu, N. M., Uçar, Y., & Esen, A. (2021). Finite difference method combined with differential quadrature method for numerical computation of the modified equal width wave equation. *Numerical Methods for Partial Differential Equations*, 37(1), 690-706. `https://doi.org/10.1002/num.22547`

[19] Başhan, A., Uçar, Y., Yağmurlu, N. M., & Esen, A. (2016, October). Numerical solution of the complex modified Korteweg-de Vries equation by DQM. In Journal of Physics: Conference Series (Vol. 766, No. 1, p. 012028). IOP Publishing. `https://doi.org/10.1088/1742-6596/766/1/012028`

[20] Bellman, R., Kashef, B. G., & Casti, J. (1972). Differential quadrature: a technique for the rapid solution of nonlinear partial differential equations. *Journal of Computational Physics*, 10(1), 40-52. `https://doi.org/10.1016/0021-9991(72)90089-7`

[21] Bellman, R., Kashef, B., Lee, E. S., & Vasudevan, R. (1975). Differential quadrature and splines. *Computers & Mathematics with Applications*, 1(3-4), 371-376. `https://doi.org/10.1016/0898-1221(75)90038-3`

[22] Quan, J. R., & Chang, C. T. (1989). New insights in solving distributed system equations by the quadrature method-I. Analysis. *Computers & Chemical Engineering*, 13(7), 779-788. `https://doi.org/10.1016/0098-1354(89)85051-3`

[23] Quan, J. R., & Chang, C. T. (1989). New insights in solving distributed system equations by the quadrature method-II. Numerical experiments. *Computers & Chemical Engineering*, 13(9), 1017-1024. `https://doi.org/10.1016/0098-1354(89)87043-7`

[24] Shu, C., & Xue, H. (1997). Explicit computation of weighting coefficients in the harmonic differential quadrature. *Journal of Sound and Vibration*, 204(3), 549-555. `https://doi.org/10.1006/jsvi.1996.0894`

[25] Shu, C., & Wu, Y. L. (2007). Integrated radial basis functions-based differential quadrature method and its performance. *International Journal for Numerical Methods in Fluids*, 53(6), 969-984. `https://doi.org/10.1002/fld.1315`

[26] Yigit, G., & Bayram, M. (2017). Chebyshev differential quadrature for numerical solutions of higher order singular perturbation problems. arXiv preprint arXiv:1705.09484.

[27] Shu, C. (1991). Generalized differential-integral quadrature and application to the simulation of incompressible viscous flows including parallel computation. University of Glasgow (United Kingdom).

[28] Shu, C., & Richards, B. E. (1992). Application of generalized differential quadrature to solve two-dimensional incompressible Navier-Stokes equations. *International Journal for Numerical Methods in Fluids*, 15(7), 791-798.

https://doi.org/10.1002/fld.16501507
04

[29] Shu, C. (2000). Differential quadrature and its application in engineering. Springer Science & Business Media.

[30] Civan, F., & Sliepcevich, C. M. (1984). Differential quadrature for multi-dimensional problems. *Journal of Mathematical Analysis and Applications*, 101(2), 423-443. https://doi.org/10.1016/0022-247X(84)90111-2

[31] Zong, Z., & Lam, K. Y. (2002). A localized differential quadrature (LDQ) method and its application to the 2D wave equation. *Computational Mechanics*, 29, 382-391. https://doi.org/10.1007/s00466-002-0349-4

[32] Tomasiello, S. (2011). Numerical stability of DQ solutions of wave problems. *Numerical Algorithms*, 57, 289-312. https://doi.org/10.1007/s11075-010-9429-2

[33] Korkmaz, A., Aksoy, A. M., & Dağ, I. (2011). Quartic B-spline differential quadrature method. *International Journal of Nonlinear Science*, 11(4), 403-411.

Meirikim Panmei *received his undergraduate degree in B.Sc. mathematics from Dhanamanjuri College, Imphal, Manipur. He has completed his M.Sc. in applied mathematics at Manipur University. He is currently a research scholar in the Department of Mathematics at Manipur University. His research interests include the differential quadrature methods and the finite difference methods.*
https://orcid.org/0009-0000-6054-1990

Roshan Thoudam *is an Assistant Professor in the Department of Mathematics at Manipur University. He completed his M.Sc. at Manipur University in 1994. He obtained his Ph.D. in numerical solutions of solitary waves based on the B-spline finite element method from the Department of Mathematics at Manipur University in 2012. His research includes differential equations, CFD, numerical methods, and scientific computing.*
https://orcid.org/0000-0001-5273-416X

An International Journal of Optimization and Control: Theories & Applications (http://www.ijocta.org)